ELSEVIER

Journal of Nuclear Materials 248 (1997) 209–213

journal of nuclear materials

Section 9. Chemical state of fission products, etc., in defected fuel pins

The chemical state of defective uranium–plutonium oxide fuel pins irradiated in sodium cooled reactors

H. Kleykamp *

Forschungszentrum Karlsruhe, Institut für Materialforschung I, Postfach 3640, 76021 Karlsruhe, Germany

Abstract

Steady-state irradiation experiments were conducted in the sodium loop of the Siloe reactor on artificially failed mixed oxide pins that had been pre-irradiated in fast reactors up to 11.5% burnup. The formation of the predominant reaction product $Na_3(U,Pu)O_4$ starts on the fuel surface and is terminated when a lower $O/(U + Pu)$ threshold of the fuel is attained. The axial extent of the reaction product depends on the size of the initial cladding defect. The occurrence of secondary cracks is possible. $Na(U,Pu)O_3$ forms at higher fuel temperatures. The existence of $Na_3U_{1-x}Pu_xO_4$ is shown in pre-irradiated blanket pins after artificial defect formation. Caesium in the oxocompounds is reduced to the metallic state and is dissolved in the coolant. Evidence of a very low chemical potential of oxygen in defective fuel pins is sustained by the occurrence of actinide–platinum metal phases formed by coupled reduction of hypostoichiometric fuel with ε-(Mo,Tc,Ru,Rh,Pd) precipitates. Continued operation of defective pins is not hazardous by easy precautions. © 1997 Elsevier Science B.V.

1. Introduction

An understanding of the chemical interactions of sodium with unirradiated and irradiated $(U,Pu)O_2$ fuel and UO_2 blanket materials is of importance in the assessment of the limits of operation of a sodium (Na) cooled fast breeder reactor (FBR). In steady-state operation the austenitic steel cladding might fail which would allow Na to enter the pin with the consequence of chemical interactions. The principle effects are that fuel, blanket and fission product fragments can be released from the failed pin into the coolant and that the Na-$(U,Pu)O_2$ reaction products can result in local swelling and overheating of the pin.

The problems of the Na-$(U,Pu)O_2$ incompatibility were recognized already in the late sixties when out-of-pile work started on the Na-fuel reaction kinetics and on the influence of the chemical potential of oxygen on the reaction behavior. This type of work was extended by a few Na-fuel capsule experiments for reaction studies under irradiation [1–9]. The field was later broadened by a property measurement program on phases in the Na–O, Na–U–O, Na–Pu–O and Na–U–Pu–O systems. The numerous physical data are now critically reviewed and compiled in [10]. The results of these programs are the basis for the chemical, mechanical and thermal modelling of defective fuel pins during irradiation and intermediate storage.

2. The Siloe irradiation program

In order to elucidate the influence of different fuel types, pin geometries, burnup of the pre-irradiation periods, defect types and defect locations on the steady-state irradiation behavior of defective fuel pins, some single-pin irradiation experiments were performed in the sodium loop of the thermal Siloe reactor at Grenoble under steady-state and moderate transient conditions within a common French–German program [5,6], see Table 1. The pins were taken from assemblies which had been pre-irradiated in the fast reactors Rapsodie, Phenix and KNK II up to 11.5% burnup at maximum linear heat ratings of 44 kW/m. The Siloe irradiations took place in the instrumented Na loop

* Tel.: +49-7247 822 888; fax: +49-7247 824 567.

0022-3115/97/$17.00
PII S0022-3115(97)00120-7

Table 1
Defective pin irradiations in the Siloe reactor

Expmt.	ρ_{fuel}	Pin diam.	Pre-irradiation		Defect		Fuel loss	Cs-137 loss
			burnup	reactor	type	location		
S 2	87%	6 mm	0 %	–	open slit	hot end	40 mg	(40 %)
S 4	87%	6 mm	9.5 %	Rapsodie	open slit	hot end	1500 mg	81 %
S 3	87%	6 mm	10.4%	Rapsodie	Zn soldered slit	hot end	130 mg	85%
RS 1	97%	8.65 mm	11.5%	Rapsodie	pre-def. slit	hot end	60 mg	92%
RS 5	95%	8.65 mm	2.3%	Rapsodie	Zn soldered hole	hot end	0 mg	0.3%
PS 0 [a]	95%	13.4 mm	5400 MWd/t	Phenix	pre-def. slit	pin middle	0 mg	3%
PS 1	95%	8.65 mm	8.7%	Phenix	pre-def. slit	max. χ	800 mg	68%
KS 1	86	6 mm	5.7%	KNK II	pre-def. slit	max. χ	< 600 mg	20%

[a] Breeding pin; 3.2% PuO_2 and 1.5% burnup after pre-irradiation.

of the reactor for a period up to 40 days. The pin hole or slit type cladding defects were simulated by in-pile melting of the out-of-pile zinc solderings or were initiated by breaching of the grooves of the cladding walls pre-thinned down to 0.1 mm thickness by a power ramp at the beginning of the irradiation. The experimental program included delayed neutron detection (DND) monitor testing, intermediate pin examinations by neutron radiography and γ-scanning, fuel loss measurements, efficiency of cold-traps, oxygen meters, etc. The defects were detected by fission gas signals and by DND. In some experiments secondary cracks occurred. The caesium release was calculated by difference from the axial ^{137}Cs-scans. The fuel loss was estimated from the masses deposited on fuel accumulation points ('centreurs') and from γ-scanning of the empty loop after reactivation of the fissile matter. Different cold-trap designs were tested in the loop to check the oxygen gettering effect by freezing out solid oxides. These results are compiled in Table 1 together with selected pin and pre-irradiation data. The destructive post-irradiation examinations were done in the Hot Cells at Karlsruhe.

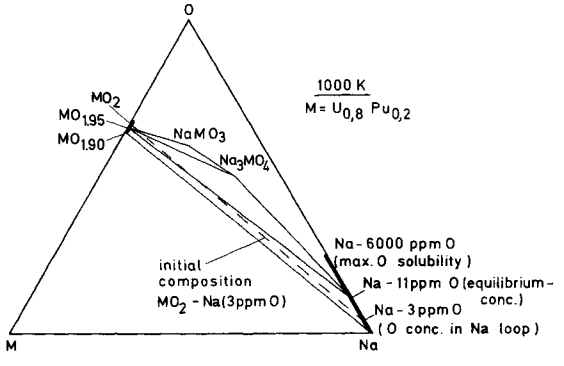

Fig. 1. Schematic isothermal section of the pseudoternary Na–$U_{0.8}Pu_{0.2}$–O system at 1000 K.

3. Results

After the defect formation of the pin, the stoichiometric or slightly hypostoichiometric mixed oxide is in direct contact with sodium containing about 3 wt.ppm oxygen that is typical for the sodium loop of an FBR. This non-equilibrium is represented in Fig. 1 by the dotted line of the schematic isothermal section of the pseudoternary Na–$U_{0.8}Pu_{0.2}$–O system at 1000 K. Reactions between fuel and coolant occur until the oxygen contents of the

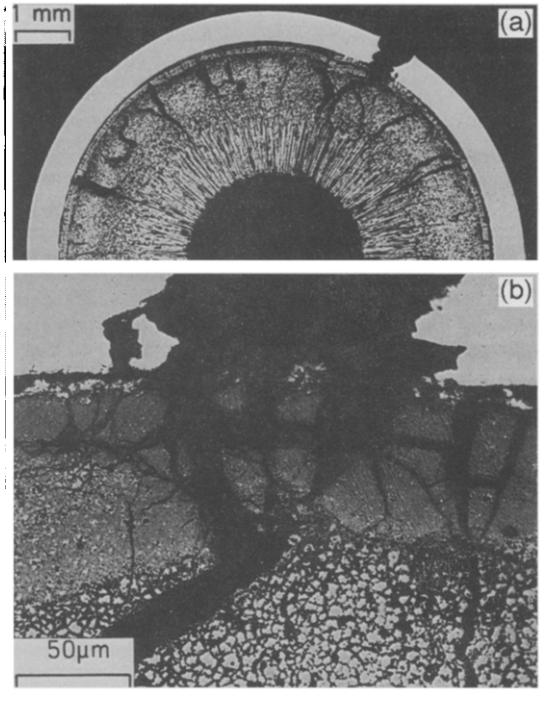

Fig. 2. Light-optical microstructure of a cross-section (a) and detail (b) in the primary defect region of the PS1 experiment.

oxide and of the sodium are adjusted to their equilibrium threshold values. The excess oxygen in the fuel is used for an increase of the oxygen concentration in the sodium and for the formation of the reaction products, e.g., $Na_3(U,Pu)O_4$, $Na(U,Pu)O_3$ and $Na_2(U,Pu)_2O_7$. The reactions come to a standstill when the fuel is reduced to the

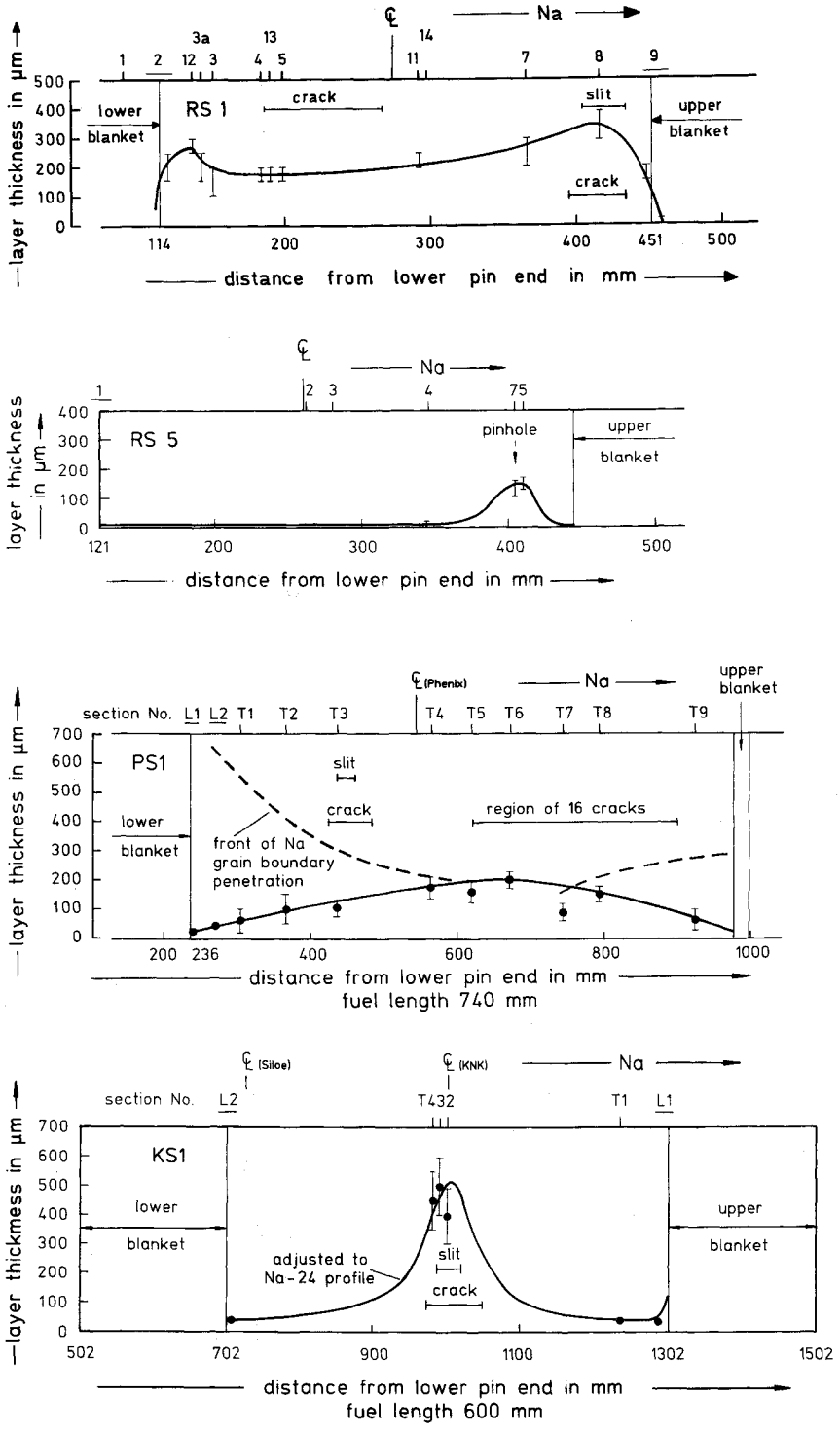

Fig. 3. Type and position of initial defects and secondary cracks and the $Na_3(U,Pu)O_4$ layer thickness between clad and fuel of selected defective pin irradiations as a function of the axial position.

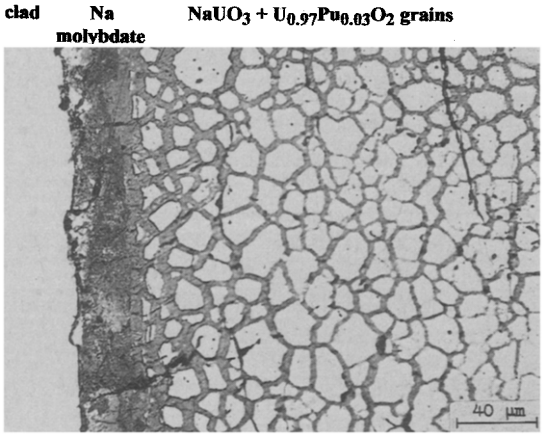

Fig. 4. Light-optical microstructure detail of a cross-section of the lower blanket of the RS1 experiment. The $U_{0.97}Pu_{0.03}O_{2-x}$ particles are covered with $NaUO_3$ reaction products; the gap is filled with Na molybdate.

strongly hypostoichiometric composition, e.g., $(U_{0.8}Pu_{0.2}O_{1.95})$ at 1000 K, which is in thermodynamic equilibrium with $Na_3(U,Pu)O_4$ and with Na containing dissolved oxygen at the threshold concentrations, e.g., 11 wt.ppm oxygen at 1000 K [10]. The average O/(U + Pu) fuel ratio is lower under realistic anisothermal conditions. A dense $Na_3(U,Pu)O_4$ layer is formed in the entire azimuth of the fuel surface at the beginning in the initial defect region. The U/Pu ratio of the reaction product is equal to or slightly higher than that of the adjacent fuel, see Fig. 2. The reaction starts from the fuel surface by grain boundary penetration of Na. The thickness of the dense reaction layer is ideally single-phase and increases with the root of time. However, residuals of $(U,Pu)O_{2-x}$ grains are visible in the $Na_3(U,Pu)O_4$ matrix which have not yet fully reacted with Na. The bulk diffusion of Na through the formed $Na_3(U,Pu)O_4$ reaction layer is the rate determining step. The chemical diffusion coefficient is $\tilde{D}_{Na} = 5 \times 10^{-6} \exp(-Q/RT)$ m^2/s with an activation energy $Q = 166$ kJ/mol between 800 and 1500 K [10]. It is assumed that $Na_3U_{1-x}Pu_xO_4$ with x up to 0.3 is in equilibrium with Na and $U_{0.7}Pu_{0.3}O_{1.95}$ [11].

The specific volume of the reaction product is about twice of that of $(U,Pu)O_2$. This causes pin swelling and secondary crack formation. Na moves axially along the gap to other positions of the pin if the initial defect exceeds a minimum area. Pin holes result in reaction product formation only in the primary defect region. The type and position of the initial defects and secondary cracks of transversal and longitudinal cuts and of the $Na_3(U,Pu)O_4$ layer thickness between clad and unreacted fuel of the defective pins RS1, RS5 and PS1 in SPX geometry and of KS1 in Mark Ia geometry are illustrated in Fig. 3.

The phase $Na_3(U,Pu)O_4$ is observed in the originally open fuel-clad gap and in the outer fuel regions along the total pin length whereas $Na(U,Pu)O_3$, U ≫ Pu, is stated in the upper (hot) pin region and in the blankets adjacent to the fuel. This behavior can be understood with the relatively low dissociation temperature of Na_3UO_4 at 1050°C whereas $NaUO_3$ is stable also at higher temperatures. Fig. 4 illustrates the microstructure of the disintegrated lower blanket adjacent to the fuel column. $U_{0.97}Pu_{0.03}O_{2+x}$ has developed from UO_2 during the pre-irradiation period. $NaUO_3$ forms by reaction of Na with this mixed oxide and covers the residual blanket particles. The outer part of the gap is filled with Na molybdate that forms by the reaction Na + Cs molybdate = Cs + Na molybdate; Cs metal also occurs by the reduction of Cs uranate, both reactions due to the strong decrease of the oxygen partial pressure after the defect formation. Cs is washed off by Na into the loop.

A blanket pin assembly with depleted UO_{2+x} was irradiated in the Phenix reactor up to a burnup of 1.5% calculated from the fission product inventory. The further irradiation of one defected pin revealed the formation of a

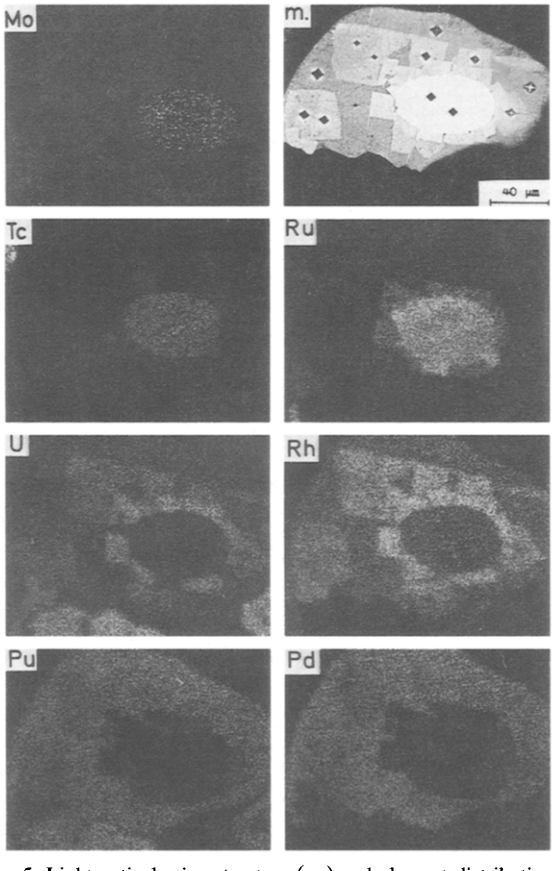

Fig. 5. Light-optical microstructure (m.) and element distribution images of a multi-phase ingot in the central void of the S3 experiment illustrating the actinide–platinum metal phase formation by coupled reduction of the fuel and the ε-phase at low oxygen partial pressure.

Na uranate according to the reaction $U_{0.953}Pu_{0.032}FP_{0.015}O_{2+x} + Na \rightarrow U_{0.953}Pu_{0.032}FP_{0.015}O_{1.995} + Na_3U_{0.965}Pu_{0.035}O_4$ + fission products (FP). The observed lattice parameters of the oxides are $a = 546.8$ pm and $a = 476$ pm, resp.

Evidence of the very low $O/(U + Pu)$ ratio of the mixed oxide after the defect formation is sustained by the occurrence of metallic precipitates, e.g., $(U,Pu) \cdot (Ru,Rh,Pd)_3$, $(U,Pu)_3 \cdot (Ru,Rh,Pd)_4$ and $(U,Pu)Sn(Rh,Pd)_2$, by coupled reduction of hypostoichiometric fuel with the ε-(Mo,Tc,Ru,Rh,Pd) precipitates formed in the pre-irradiation period of the pin. Ru plays a minor role in these actinide–platinum metal phases. The reaction takes place, e.g., according to the equation $(Mo,Tc,Ru,Rh,Pd) + (U,Pu)O_{2-x} \rightarrow (Mo,Tc,Ru) + (U,Pu) \cdot (Rh,Pd)_3 + (U,Pu)O_{2-x+\varepsilon}$, $\varepsilon \ll 1$. A multiphase ingot is illustrated in Fig. 5. The reactions are explained by the low chemical potential of oxygen in the fuel and by the high thermodynamic stability of the formed intermetallic phases, $\Delta_f G^0(URh_3) = -286$ kJ/mol [12] and $\Delta_f G^0(UPd_3) = -312$ kJ/mol [13] at 1323 K. These phases are insoluble in nitric acid.

The maximum $Na_3(U,Pu)O_4$ layer thickness is located in the primary defect region of the pins. The radial plutonium enrichment at the central void of the fuel pins created during the pre-irradiation period is not further increased during the defective pin irradiation. The bulk density of the fuel has no influence on the extent of the Na uranoplutonate layer formation. Fuel loss increases with increasing open area of the cracks. However, it is obviously reduced by tight $Na_3(U,Pu)O_4$ layers on the surface of the defect and secondary crack regions. $Na_3(U,Pu)O_4$ formation is mitigated in defective pins by use of hypostoichiometric fuel with an initial O/M fuel ratio $\simeq 1.96$, by effective cold-traps for oxygen gettering in the Na coolant and by about 50% power reduction of the reactor immediately after the defect detection.

4. Conclusions

The technological conclusions of the French–German defective mixed oxide fuel pin irradiation program in the Siloe reactor are as follows:

(1) Fuel loss appears predominantly directly after the defect formation.

(2) Fuel loss increases with the geometric crack area.

(3) No quantitative correlation was observed between recoil area (DND signal) and mass of fuel loss into the sodium loop.

(4) No fuel loss was found when the DND signal is < 1 cm^2 recoil.

(5) Parabolic rate law of $Na_3(U,Pu)O_4$ layer formation; reaction is stopped when $O/(U + Pu)$ fuel ratio is reduced to a lower threshold.

(6) Fuel density has no influence on the extent of the $Na_3(U,Pu)O_4$ formation.

(7) No pin-to-pin failure propagation (inferred from pin bundle experiments).

(8) Continued operation of defective pins by about 50% linear heat rating reduction.

(9) Use of low $O/(U + Pu)$ fuel and effective oxygen gettering by cold traps after defect detection are recommended.

References

[1] P.E. Blackburn, A.E. Martin, J.E. Battles, P.A.G. O'Hare, W.N. Hubbard, Proc. Conf. on Fast Reactor Fuel Element Technology, New Orleans, USA, 1971, p. 479.
[2] M. Hosseau, J.F. Marin, F. Anselin, G. Déan, Proc. Symp. on Fuel and Fuel Elements for Fast Reactors, Vol. 1, Brussels, Belgium, 1973, p. 277.
[3] M.G. Adamson, GEAP-12519, 1974.
[4] M.G. Adamson, E.A. Aitken, D.W. Jeter, Proc. Int. Conf. on Liquid Metal Technology in Energy Production, Champion, USA, 1976, p. 866.
[5] A. Chalony, M. Conte, J. Perves, J. Veyrat, H. Miemczyk, H. Plitz, P. Weimar, Proc. Int. Meeting on Fast Reactor Safety Technology, Seattle, USA, 1979, Vol. 5, p. 2440.
[6] H. Plitz, G.C. Crittenden, A. Languille, J. Nucl. Mater. 204 (1993) 238.
[7] M.A. Mignanelli, P.E. Potter, J. Nucl. Mater. 125 (1984) 182.
[8] M.A. Mignanelli, P.E. Potter, J. Nucl. Mater. 130 (1985) 289.
[9] R. Lorenzelli, T. Athanassiadis, R. Pascard, J. Nucl. Mater. 130 (1985) 298.
[10] H. Kleykamp, KfK-4701, 1990.
[11] S. Pillon, CEA-R-5489, 1989.
[12] H. Kleykamp, Pure Appl. Chem. 63 (1991) 1401.
[13] H. Kleykamp, S.G. Kang, J. Nucl. Mater. 230 (1996) 280.